

GRID-OPTIMIZATION FOR k - ϵ TURBULENCE MODEL SIMULATION OF NATURAL CONVECTION IN ROOMS

Niu, J. and van der Kooi, J.
Laboratory for Refrigeration & Indoor Climate Technology
Delft University of Technology
The Netherlands

ABSTRACT

This paper presents the experimental validation of numerical simulation with the k - ϵ turbulence models of the buoyancy-driven air flow in a real-sized, enclosed room. In the measurements, the flow patterns are revealed through flow visualisation technique, heat flows through enclosure surfaces are determined through energy balance calculations, and the velocity profile and turbulent-kinetic-energies in the natural convection boundary are measured by using a hot-wire anemometer. In the simulation, special efforts are placed on the examination of the influence on simulation results of grid refinement in the boundary layer close to the wall, with the standard k - ϵ turbulence model and the Lam & Bremhorst low Reynolds number turbulence model. It is found that, with the standard k - ϵ model, larger values of y^+ under-estimate the heat transfer, and vice versa. Therefore, a new optimum first grid distance is suggested for the standard k - ϵ model simulation of natural convection in rooms. It is also found that, with the low Reynolds number model, convergent solutions can be achieved only with extremely fine grids close to the heating and cooling surface, and that the consequent simulation result is reasonable. The applicabilities of the two k - ϵ models for the simulation of in-room air flows are discussed.

Keywords: k - ϵ Turbulence Model, Numerical Simulation
Natural Convection, Heat Transfer Coefficients

GRID-OPTIMIZATION OF k - ϵ TURBULENCE MODEL SIMULATION OF NATURAL CONVECTION IN ROOMS

Niu, J. and van der Kooi, J.
Laboratory for Refrigeration & Indoor Climate Technology
Delft University of Technology
The Netherlands

INTRODUCTION

The application of CFD (computational fluid dynamics) in air conditioning can be classified into following three categories: 1). system performance prediction in terms of air flow patterns, thermal-comfort and indoor-air-quality indices[1,2]; 2). building dynamics analysis through coupled simulation of the transient thermal behaviour of building envelopes and the indoor air flow patterns, for energy estimation[1,3] or for control system analysis[4]; and 3). performance of 'numerical experiments' in place of real-size experiments to obtain experimental correlations[5].

To predict the turbulence behaviour of the air flow encountered in rooms, the k - ϵ turbulence model is widely used. The k - ϵ turbulence model was developed by Launder and Spalding[6] to model fully-turbulent flows. However, flows close to a fixed wall are much determined by molecular viscous effect. In practice, one approach is to use the logarithmic wall functions in conjunction with the k - ϵ turbulence model, and empirically, the first grids used for the discretization of the differential equation are located at a certain distance from the wall. The dimensionless distance y^+ is often used to locate the first grid line. Renz *et al.*[7] studied the influence of the first grid location, and found that, by locating the first grid dimensionless distance $100 > y^+ > 40$, the simulated velocities and turbulence intensity are 25% lower and the simulated temperatures are 5% lower than the measurements in a jet ventilated room. Ozoe *et al.*[8] found that the $y^+ > 11.5$ presented wrong prediction of the heat transfer for natural convection in water, and suggested that $y^+ < 11.5$ should be used to locate the first grids. In fact, Henkes *et al.*[9] used very fine grids within the boundary layer in their simulation of turbulent natural convection in an air cavity, and higher-biased heat transfer was found. Similar conclusion was also reported by Chen *et al.*[10] in their simulation of natural convection in an air cavity. This is mainly due to the nature that the logarithmic wall functions are deduced for forced convection boundary layer flows. On the other hand, the air flow in a room is normally influenced both by forced convection and natural convection. And more often, natural convection boundary flow is formed along the window surface. Obviously, accurate simulation of the air flow and the heat transfer from the convective surfaces will have great influence on the overall prediction efficiency. Therefore, while $11.5 < y^+ < 100$ may be used for forced convection

flows near a solid wall, grid-optimization for natural convection boundary layer is also necessary for a better accuracy of heat transfer simulation.

Another approach is try to adapt the standard k - ϵ turbulence model into the boundary layer so that the wall functions can be avoided. In this category, a number of low Reynolds k - ϵ turbulence models[11] have been developed. One of the models, the Lam & Bremhorst model[12], was validated by Chen(1990) against the measurements of natural convection in a air cavity. It was found that the predicted velocity profile, turbulent kinetic energy, as well as the temperature are in better agreements with the measurements than the standard k - ϵ model. However, it was reported that extremely fine grids were used near the wall, and that converging of the iteration procedure became slower and more difficult. Obviously, this extremely fine grids requirement will limit the applicabilities of the model in practice.

In view of the fact that the k - ϵ turbulence models contain several empirical parameters, their applicability should be validated against the situation for which they are going to be used. In the present paper, measurements in a real sized room with a heating radiator and simulated cold window surface will be used to validate the k - ϵ models. Emphasis will be placed on the investigation of the effect of grid refinement in the boundary layer, and the purpose is to explore the possibility of grid-optimization for natural convection boundary layer. Besides, two different boundary conditions for k and ϵ will be compared for the Lam & Bremhorst model.

The k - ϵ TURBULENCE MODELS

The Standard k - ϵ Turbulence Model

1). Basic Equations

This model is based on the Reynolds Time-Average Navier-Stokes equations and the Boussinesq turbulent viscosity hypothesis. All the equations in this model read in the general form

$$\Delta(\rho U\Phi - \Gamma_{\Phi,eff}\nabla\Phi) = S_{\Phi} \quad (1)$$

where, $\Gamma_{\Phi,eff}$ is the effective diffusion coefficient, ρ is fluid density, U is the velocity vector, Φ can be any of the physical quantities of velocity components u_i , enthalpy H , turbulent-kinetic-energy k , or turbulent-energy-dissipation-rate ϵ . The corresponding constants and coefficients of the individual equations are summarized in Table 1. In our study, the standard values of the empirical constants in the k - ϵ model, as recommended by Launder and Spalding[6], were used.

2). Boundary Conditions

With the standard k - ϵ turbulence model in the program PHOENICS, the logarithmic wall functions are used[13]. In the program, the skin friction factor is first calculated

Table 1 Terms, Coefficients and Constants in Equation(1)

Φ	$\Gamma_{\Phi,eff}$	S_{Φ}
1(Continuity)	0	0
u_i	μ_{eff}	$-\partial p / \partial x_i - \rho \beta / C_p g_i \theta$
k	μ_{eff} / σ_k	$G - \rho \epsilon + G_B$
ϵ	$\mu_{eff} / \sigma_{\epsilon}$	$[\epsilon(C_1 G - C_2 \epsilon) / k] + C_3 \epsilon / k G_B$
H	μ_{eff} / σ_H	S_H
$G = \mu_i (\partial u_i / \partial x_j + \partial u_j / \partial x_i) \partial u_i / \partial x_j$ $G_B = \beta / C_p \cdot g_i \mu_i / \sigma_{H,t} \cdot \partial \theta / \partial x_i$ $\theta = H - H_0$ $\mu_{eff} = \mu_t + \mu$ $\mu = C_{\mu} \rho k^2 / \epsilon$ $C_1 = 1.44, C_2 = 1.92, C_3 = 1.44, C_{\mu} = 0.09, \sigma_k = 1.0, \sigma_{\epsilon} = 1.3, \sigma_H = 0.9$		

from the formula

$$S = \left[\frac{0.435}{\ln(1.01 + 9Re \cdot S^{0.5})} \right]^2 \quad (2)$$

where $Re = uv/y_p$, y_p is the distance of the first grid node from the wall.

To calculate the convective heat transfer from the solid wall, the Stanton number is calculated from

$$St = \frac{S}{Pr_t (1.0 + P \cdot S^{0.5})} \quad (3)$$

where

$$P = 9.0 \times (Pr_t / Pr_l - 1.0) \cdot (Pr_t / Pr_l)^{0.25}$$

and Pr_l and Pr_t are the laminar and turbulent Prandtl numbers respectively.

For the k and ϵ equations, the boundary conditions are fixed by the following two formulas

$$k_p = \tau / (\rho C_{\mu}^{0.5}) \quad (4)$$

and

$$\epsilon_p = \frac{(\tau / \rho)^{1.5}}{0.41 y_p} \quad (5)$$

where τ , is the skin shear stress.

Low-Reynolds-number k-ε Model

1. Basic Equations

To adapt the k-ε concept to boundary flows, a number of modifications have been made to the standard k-ε model, and therefore a number of so called low-Reynolds number models are developed. In these low-Reynolds number models, several functions are introduced into the k and ε equations:

$$u \frac{\partial k}{\partial x} + v \frac{\partial k}{\partial y} = \frac{\partial}{\partial x} \left(\nu + \frac{\nu_t}{\sigma_k} \right) \frac{\partial k}{\partial x} + P_k - \varepsilon + D$$

$$u \frac{\partial \varepsilon}{\partial x} + v \frac{\partial \varepsilon}{\partial y} = \frac{\partial}{\partial x} \left(\nu + \frac{\nu_t}{\sigma_\varepsilon} \right) \frac{\partial \varepsilon}{\partial x} + (C_{\varepsilon_1} f_1 P_k - C_{\varepsilon_2} f_2 \varepsilon) \varepsilon / k + E \quad (7)$$

There are different forms of functions for f_1 , f_2 , f_μ , D and E in different low Reynolds number models[11]. In our study, only the Lam and Bremhorst model was investigated. The above functions in this model are:

$$f_\mu = (1 - \exp(-0.0165 Re_\mu))^2 (1 + 20.5 / Re_\mu)$$

$$f_1 = 1 + (0.05 / f_\mu)^3$$

$$f_2 = 1 - \exp(-Re_\tau^2)$$

$$D = E = 0$$

2. Boundary Conditions

For low Reynolds number k-ε models, no wall functions are required for boundary conditions. However, boundary conditions for k and ε must be specified in one form or another. For Lam & Bremhorst model, there are at least four different forms of wall boundary specification reported[8,9,10]. In our study, the following two approaches will be studied.

1). boundary specification I[8,9]

$$k_w = 0, \quad \varepsilon_w = 2 \nu k / y^2 \quad (8)$$

i.e., the turbulent kinetic energy at the wall is assumed to be zero, while the dissipation rate of turbulence energy is calculated according to Eq.(8).

2). boundary specification II

The logarithmic law wall function is still used. However, different from the standard k-ε model, the grid lines can be and should be located in the viscous sub-layer. This practice was reported in Ref[10].

In principle, both the boundary condition specifications require that, at least the first grid

line be located in the viscous sub-layer. It can be expected that finer grids are needed in the low Reynolds number turbulence model than in the standard k- ϵ model.

Numerical Schemes

The computer program PHOENICS is used in the present calculation. The underlying numerical scheme is as follows. The differential equations of momentum and enthalpy are discretized by finite-volume method. The 'staggered grid' was introduced in the program PHOENICS, and for the convection term, the up-wind scheme was used. The continuity equation is taken into account by solving the pressure-correction equation. The overall solution procedure is an iteration process, which is similar to the procedure SIMPLE[14], which stands for Semi-Implicit Method for Pressure-Linked Equations.

EXPERIMENTAL INVESTIGATIONS

In a most recent paper[15], experiments on convection heat transfer in enclosures are reviewed. Altmayer *et al*[5] used 'numerical experiments' and investigated several combinations of heating and cooling enclosure sub-surfaces. Of particular interest to the author, is the correlation about the natural convection heat transfer along a vertical hot plate in an isothermal environment

$$h=0.13(Gr\cdot Pr)^{0.33} \quad (9)$$

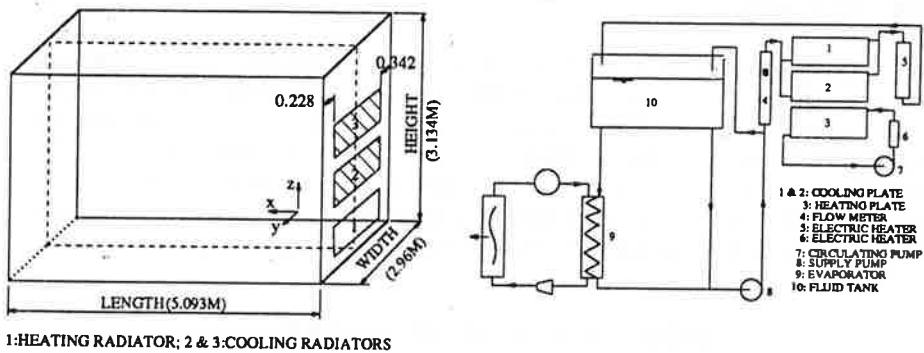
Altmayer's result has shown that the correlation is also valid for the 'most hot' subsurface when the adjacent subsurface temperatures are close to the air temperature. Therefore, for our purpose, the correlation will be used as a reference for the measurements of convection heat transfer in the climate room.

Experimental Set-up and Instrumentation

The measurements were done for the natural convection in a real-size, enclosed room. The configuration of the room is shown in Fig.1a). Three plate radiators are located at the end wall of the room, with the upper two cooled and the lower one heated. A plank wood of 250mm in width is located horizontally between the heating and cooling plates to simulate a window sill, to avoid the oscillation of the flow patterns.

The surface temperature of the heating plate, T_H , can be maintained at a certain temperature in the range of 25°C to 60°C, and that of the cooling plate, T_C , 10°C to 20°C, while the room average temperatures, T_r , are balanced at about 25°C. The other enclosure surface temperatures are actively regulated so that near-adiabatic conditions are maintained. The temperature differences, $\Delta T_H = T_H - T_r$ and $\Delta T_c = T_r - T_C$, will determine the eventual flow patterns. As we know, natural convection can be described by two dimensionless parameters, the Grashof number(Gr) and Prandtl number(Pr). In the present study, $Gr = 10^8 - 10^9$, which is typical in real rooms. The heating plate was heated by an electric heater in the circulating flow circuit, the supply power of which

are measured by a watt-meter, while the cooling plates are cooled by the glycol/water mixture from a chiller, as shown in Fig.1b).



a). Configuration of the Test Room

b). Flow Diagram of Cooling & Heating Systems

Fig. 1

The middle vertical plane (illustrated in Fig. 1) of the room was lit by a planar-light source. The air flow in the middle plane were visualised through the movement of the smokes, generated by a smoke machine. A video-camera was used to take pictures of the motion.

A number of thermocouples are attached on all of the internal enclosure surfaces to measure the surface temperature, with six thermal-couples on each of the heating and cooling surfaces. Also in the middle vertical plane, 20 thermal couples are located to measure the air temperature.

Experimental Results

1. Visualised Flow Patterns and Measured Temperatures

Shown in Fig.2 are drawings of the visualised flow patterns at several different temperature conditions. As expected, an upward-flow and downward-flow were initiated by the heating and cooling plates, respectively. The two streams meet at certain height, subsequently change their direction and a converged outward-flow is formed at the meeting point. The converged-flow turns into a horizontal flow 'jet', enhanced by the horizontally-placed window-sill. This jet is further biased upward or downward, depending on the relative temperature differences.

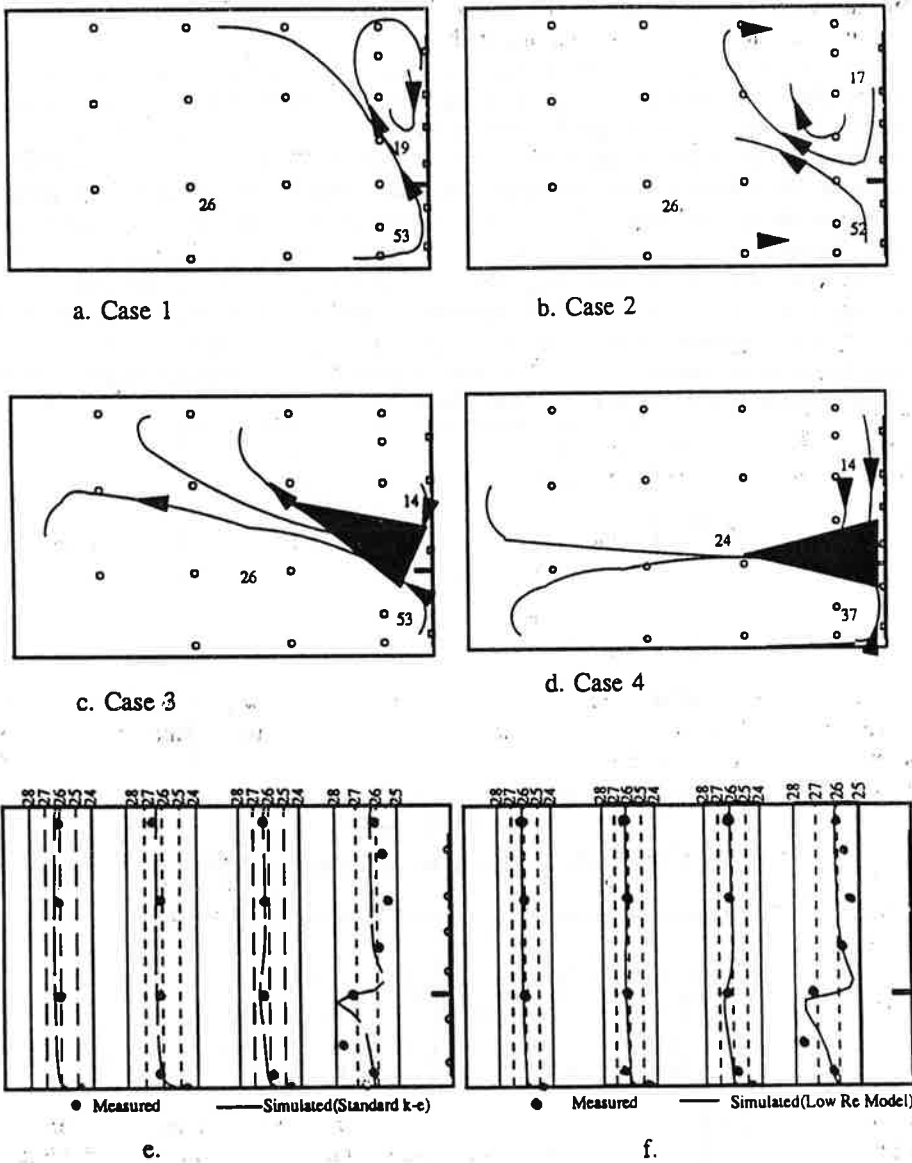


Fig. 2. Flow patterns and temperature profiles in the middle plane
 (sub-figures e. and f. are the measured air temperature profiles along the four vertical lines in the mid-plane of Case 3, with the simulated results by the standard k-ε model and the low Reynolds number model respectively)

2. Heat Flow Measurements

The overall heat supply to the heating plate is taken to be equal to the supplied power to the electric heater, Q_H plus the mechanical energy contribution from the circulating pump. With the surface temperatures measured, the radiant heat exchanges were obtained by calculation, taking into account the multi-reflectance between the enclosure surfaces. The convection heat flow from the plate is obtained by subtracting the radiant part from the overall supply. The convection heat transfer coefficients h is calculated from the equation $\alpha = Q_c / A \cdot \Delta T_H$, where A is the surface area of the plate and ΔT_H is the temperature difference between the surface concerned and the room air average. Shown in Fig.3, are the convection heat transfer coefficients h measured for different temperature conditions. Also plotted in the chart, is a curve of correlation which is for natural convection around an 'isolated' vertical plate[5]. The measured values of h are slightly higher than those from the correlation.

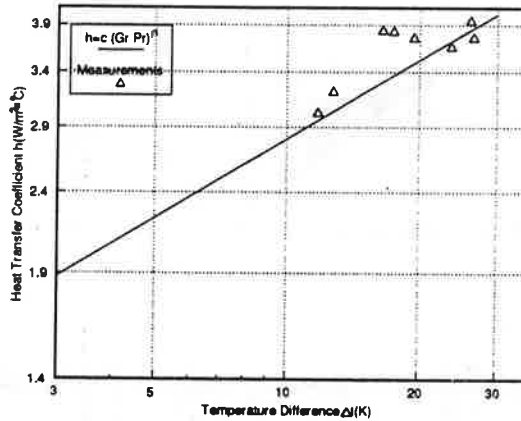


Fig.3 Measured convective heat transfer coefficients

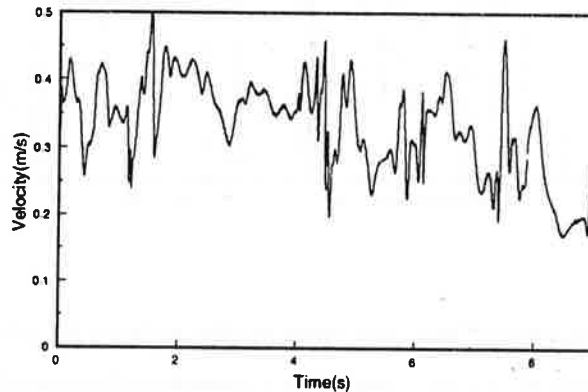


Fig.4. Velocity fluctuations at one of the measurement points

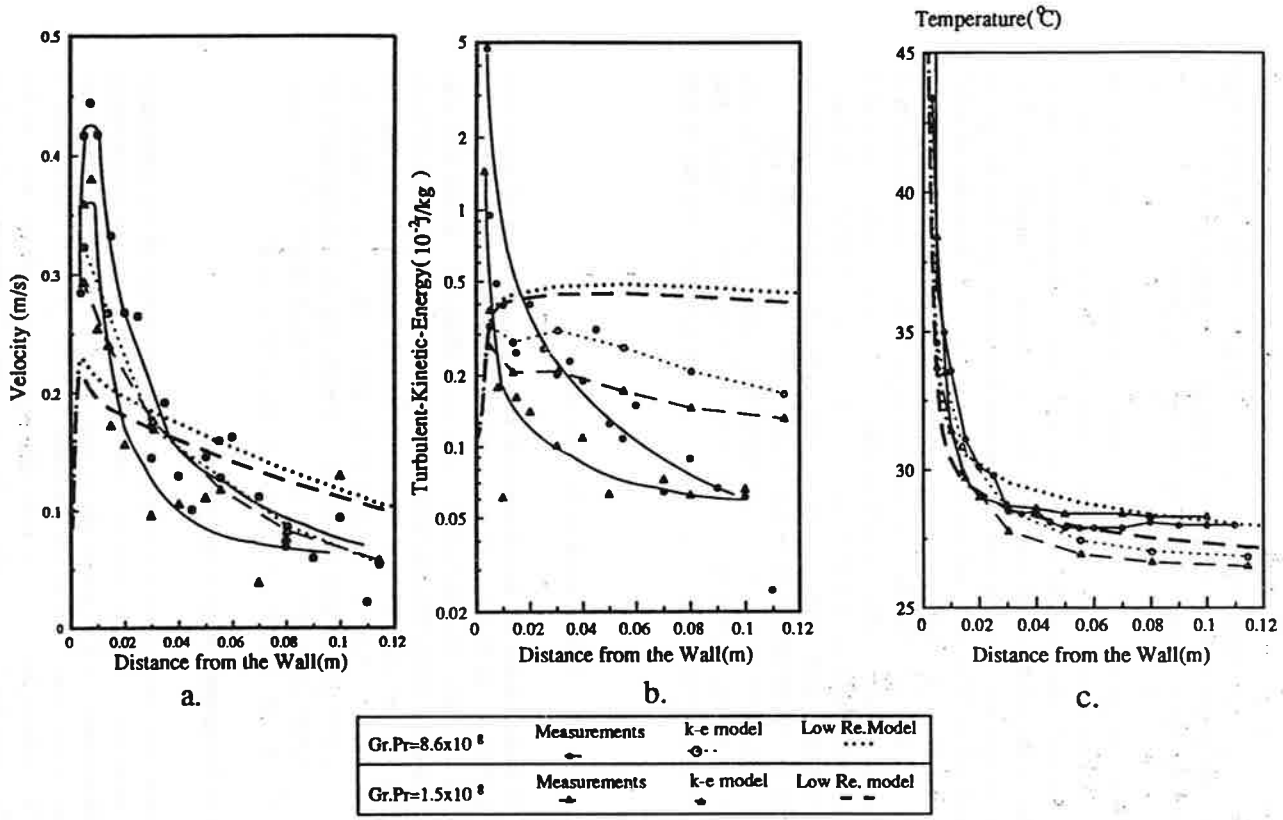


Fig. 5. Measured and simulated velocity, turbulent kinetic energy, as well as the temperature profiles of the boundary layer flow

3. Boundary-Layer Measurements

A DISA anemometer was used to measure the local velocities close to the heating plate. The anemometer was first calibrated in a small scale wind-tunnel at five different fluid temperatures. In measurements, temperatures were measured simultaneously so that the influence of the temperatures could be corrected through calculation.

The measurements were done at two height positions, 375mm and 750mm from the floor respectively, for the heating plate. The corresponding Grashof numbers are 1.5×10^8 and 8.6×10^8 , respectively. An example of the monitored velocity fluctuations is shown in Fig.4, measured at the height corresponding with $Gr \cdot Pr = 8.6 \times 10^8$ and 20 mm away from the surface. A high speed datalog was used to take data at the speed of 250 points per second for a period of 20 seconds and the data were stored in the hard-disc of a PC. Mean velocities as well as the turbulent kinetic energies were worked out afterwards. The results are shown in Fig. 5. The data are scattered around due to random errors in measurements, but the velocity profile can still be seen. The velocity profile agrees with Hammond's analysis[16] that a plane wall jet consists of three layers: the outer turbulent layer, the inner turbulent layer and the viscous sub-layer. The position where the maximum velocity lies is considered to be the boundary between the outer and inner turbulent layers. The thickness of a buoyancy-driven turbulent boundary layer is defined as the distance of the maximum velocity position from the wall. This distance is less than 10mm in our measurements. Compared with the scale of the room, this size is very small.

SIMULATION RESULTS

For the purpose of investigating the performance of simulation in terms of prediction accuracy, different y^+ values of the first grid were tested for the standard k- ϵ model with the logarithmic wall functions. The performance of Lam & Bremhorst model was also tested. In all the simulation cases, the measured enclosure surface temperatures of Case 3 (indicated in Fig.3c) are used for the thermal boundary conditions, so that the experimental result from the measurements can be used directly to validate the simulation results. The average surface temperature of the heating and cooling plates are 52.6°C and 14.5°C, respectively, and the ceiling and wall temperature 25.6°C, floor temperature 24.5°C. Details of these simulations are described as below.

The Standard k- ϵ Turbulence Model Simulations

First, six simulation cases are conducted to examine the sensitivity of the simulation results to the distance of the first grid line. In these cases, the simulation is conducted only in the 2-dimensional X-Z vertical plane and the grid coarseness has been determined in such a way that, close to the enclosure surface, the node distribution is denser than in the central domain. The only difference among these cases is the distances of the first grid-line from the plates. In these cases, the distances of the first grid-nodes are 0.625mm, 1.25mm, 2.5mm, 5mm, 9mm and 20mm, respectively. It is found that this first distance has a remarkable influence on the simulation results, in

respect of the simulated flow patterns, temperature distributions and especially the predicted convection heat transfer coefficients. The resulting dimensionless distance y^+ of the first grid-line is calculated for each case, and it is found that the y^+ value varies, along the heating plate, from 5.0 to 7.4, 8.1 to 10.3, 10.2 to 13.0, and 14.2 to 16.8 in each of the simulation cases. The predicted heat transfer coefficients in each case are plotted against the maximum dimensionless distance y^+_{max} in Fig. 6. It can be seen that a smaller y^+ value over-estimates the h value, and vice versa. In other words, the predicted h is rather sensitive to the y^+ value. By interpolation, it can be expected that the predicted h value would be closer to the measured value if y^+_{max} is equal to 9.2. Therefore, if the y^+_{max} is used as a criterion to locate the first grid lines, the optimum value is $y^+_{max,opt} = 9.2$. This requirement is different from that for forced convection boundary layers. Much finer grids should be used next to the wall for natural convection, and also the optimum value range is much smaller.

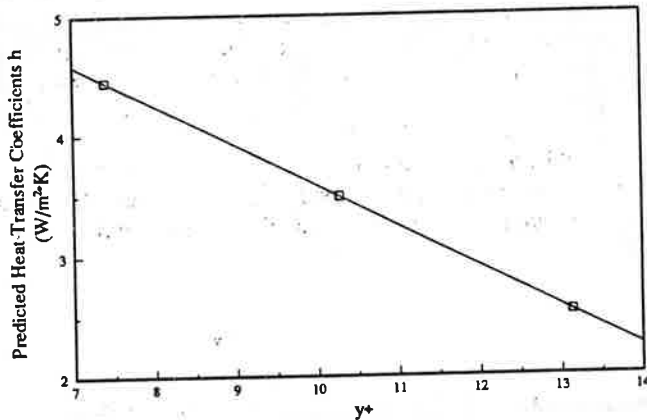


Fig. 6. Dependence of the simulated h on the first grid dimensionless distance

Then, a three dimensional simulation is conducted. The grid number used is $NX \times NY \times NZ = 25 \times 22 \times 30$. The graphics results of the simulation are shown in Fig. 7. The simulated velocity vectors in the middle plane (Fig. 7a) can be compared with the visualised flow pattern (Fig. 2c). In terms of the angles of the converged 'jet' and the relative sizes of the two recirculation zones, the simulated flow pattern is reasonable. Also, both measured and simulated temperature profiles along the four vertical lines in the mid-plane are plotted in Fig. 2e. It can be seen that the agreement is good farther away from the plates, while larger discrepancy exists closer to the plates.

Some local values (close to the heating plate) of the predicted velocity and turbulent kinetic energy, as well as the temperatures are plotted in Fig. 5, to be compared with the anemometer measurements. The mean velocity and temperature agreement is reasonable, while greater discrepancies exist for turbulent kinetic energies. The predicted convection heat transfer is very close to the measurements, and the nominal transfer coefficient, calculated from the temperature difference of the heating plate surface and

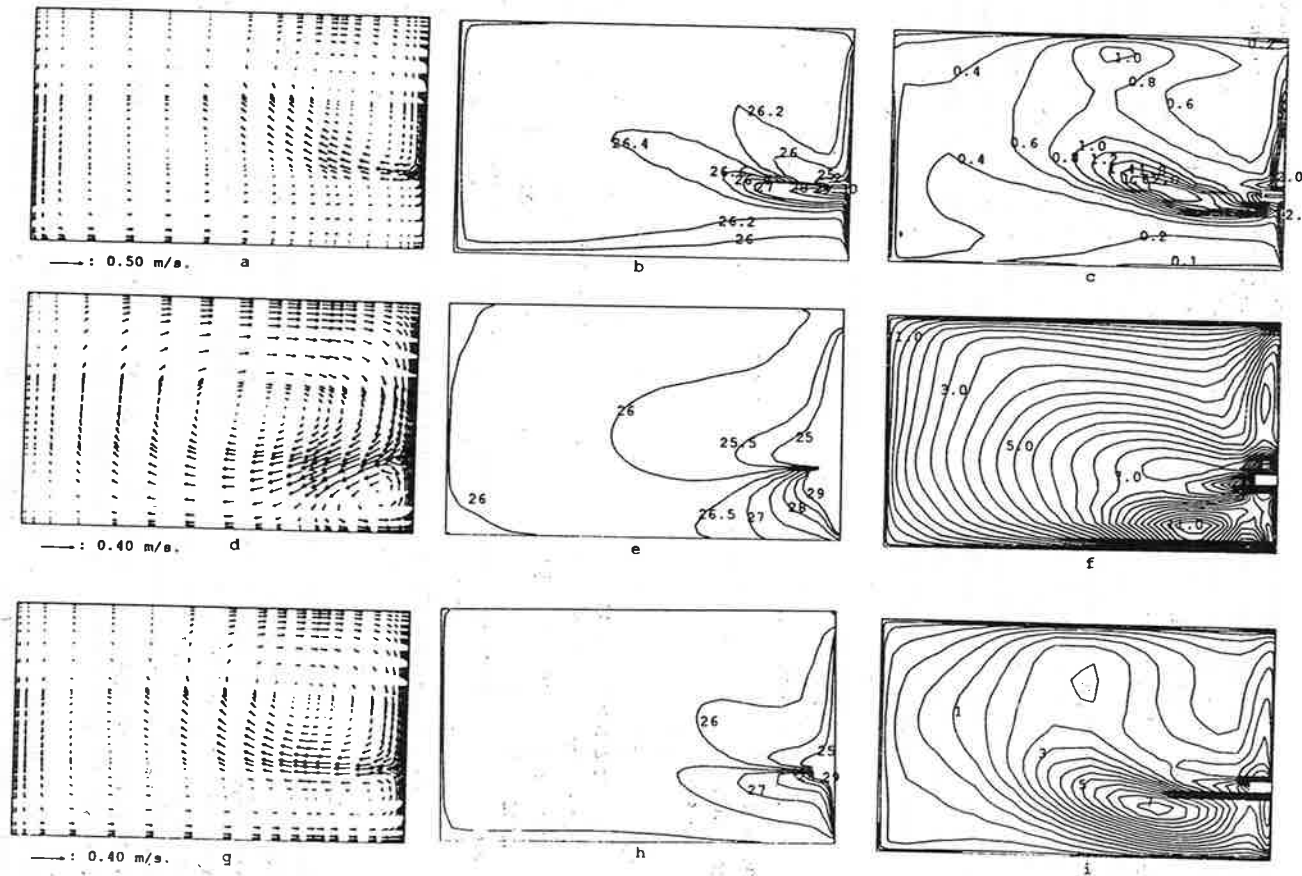


Fig. 7. Comparison of simulated results by different turbulence models
 a-c: the standard k- ϵ turbulence model + logarithmic wall functions; d-f: Lam & Bremhorst model + Eq. (8); g-i: Lam & Bremhorst model + logarithmic wall functions; Figures in the 1st column are velocity vectors, 2nd column isotherms($^{\circ}\text{C}$), 3rd column contours of turbulent kinetic energy(10^3J/kg)

the room-air average, is $3.59 \text{ W/m}^2\cdot\text{K}$, which is slightly lower than the measured value (about $3.7 \text{ W/m}^2\cdot\text{K}$). In comparison with the measured velocity profile of the boundary flow (Fig.5a), the grid cells of the first line are located just within the inner boundary layer. Post-check shows that the y^+ values of the grid line next to the heating plate are in the range of 8.1 and 10.0. This agrees with the 2-dimensional analysis above.

Performance of Lam & Bremhorst Low Reynolds Number Model

1. With boundary conditions for k and ϵ as described in Eq.(8), different grid-fineness in the boundary layer close to the wall are tested. It was found that, only with the finest grid tested, a converged solution was achieved. However, the predicted heat flow from the heating plate is 300% of the measurement. In comparison with the visualised flow pattern(Fig.2c), the size of the upper recirculation zone of the air flow is much over-predicted(Fig.7d), while that of the lower recirculation zone is under-predicted.

In comparison with the standard k - ϵ model prediction(Fig.7a), the predicted temperature variations of the room air(Fig.7e) are larger. Also the predicted k (Fig.7f) is about 10 times higher. In summary, this prediction is far from reliable. Since almost 10 grid lines were already located within the 10 mm range near wall region, no further refining of grids was tested.

2. The logarithmic wall functions are still used with the low Reynolds number model. The same grid fineness is tested. It was found that, no converged solution can be found with coarse grids in the near wall region. During the iteration process, the predicted heat flow oscillates in a certain range around the level that is close to the measurements. The predicted k tends to be zero in most region, except in the region close to the heating and cooling surfaces and in the region where the two streams meet. Again, a converged solution is achieved only with the finest grids tested. In this case, the comparison with measurements is encouraging. The simulated flow pattern is reasonable (Fig. 7g). The simulated temperature contours(isotherms) of room air (Fig. 7h) are similar with the standard k - ϵ simulation (Fig.7b). Important is that the predicted heat flow is within the error range of the measurements.

On the other hand, the agreements of local velocities and turbulent kinetic energies with measurements of the near wall region are no better than those from the standard k - ϵ model (Fig. 5 a and b), though the temperature agreement looks better in the plotting (Fig.2f and Fig.5c). The low Reynolds number model tends to predict higher k values - about 3 times of the standard k - ϵ model predictions (Fig. 7i). But both models fail to predict the peak values of k close to the plate, which were found in the measurement (Fig.5b).

CONCLUSIONS AND DISCUSSIONS

1). Applicability of the standard k - ϵ Turbulence Model

The predicted flow pattern as well as the temperature distribution can be in reasonable

agreement with experimental investigations. However, it is found that the prediction results, especially the convection heat transfer next to the wall is very dependent on the dimensionless distance y^* of the first grid, when the built-in wall functions are used. The optimum y^*_{max} found to be around the value 9.2. It must be noted that this optimum y^* is different for forced convection and natural convection situations.

In air conditioned rooms, unfortunately, forced convection and natural convection play compatible roles in the flow, heat transfer, as well as the mass transfer processes. Therefore, careful attention should be paid to the grid optimisation in simulation. The convection nature along the individual enclosure surfaces should be analyzed in advance, and different grid sizes are used for the different surfaces. It is suggested that empirical convection heat transfer data be used when available, which can lead to more reliable results, especially when the flow parameter and air contaminant distributions in the occupied zone are of interest of the simulation.

2). Application of low Reynolds No. $k-\epsilon$ Models

In principle, the low Reynolds No. model can eliminate the first-grid-dependent characteristics of the standard $k-\epsilon$ model, as long as the grids are fine enough within the boundary layer. In fact, it was found in the present study that, when less than 8 grid cells are located in the boundary layer, no converged results could be obtained. It seems that the Lam & Bremhorst model only works when extremely fine grids are located in the near wall region. Also, the logarithmic wall functions should be used, purely on empirical basis. In comparison with the equivalent standard $k-\epsilon$ model simulation, about 2 or 3 times CPU time will be required on a SUN work-station.

ACKNOWLEDGEMENT

The authors wish to thank Messrs Aad van Geest, Herman F. Broekhuizen and Martin Verwaal for their help in the experimental measurements, and Messrs Arie Visser and Rob Staal for their help in running the computer code PHOENICS. Special thanks are given to Dr. Q. Chen for his help in using the computer code PHOENICS. Special thanks are also given to Mr. C. Gerritsen of Laboratory for Aero- and Hydro-Dynamics, TU Delft for lending us their anemometer apparatus.

REFERENCES

- [1] Chen, Q., J. van der Kooi, and A. Meyers, Measurements and Computations of Ventilation Efficiency and Temperature Efficiency in a Ventilated Room, *Energy and Buildings*, Vol.12, No.2, 1988, pp.85-99
- [2] Chen, Q., P. Suter, and A. Moser, Evaluation of Indoor Air Quality by a Perceived Comfort Equation, *Proc. of Conference on Indoor Air Quality and Climate: Indoor Air'90*, July 29 - August 3, 1990, Toronto, Canada
- [3] Chen, Q. and J. van der Kooi, A Methodology for Indoor Air Flow Computations and Energy Analysis for a Displacement Ventilation System, *Energy and Buildings*, Vol.14, 1990, pp.259-271

- [4] Holmes, N. J., J. K-W Lam, K. G. Ruddick, and G. E. Whittle, Computation of conduction, convection and radiation in the perimeter zone of an office space, *Proc. of ROOMVENT-90*, Oslo, June, 1989
- [5] Altmayer, E.F., A.J. Gadgil, F.S. Bauman, & R.C. Kammerud, Correlations for Convective Heat Transfer from Room Surfaces, *ASHRAE Transactions*, V.89, 1983, Pt.2A, pp.61-77
- [6] Launder, B. E. and D. B. Spalding, The Numerical Computation of Turbulent Flow, *Comp. Methods Appl. Mech. Eng.*, Vol. 3, 1974, p.269.
- [7] Renz, U. and U. Terhaag, predictions of air flow pattern in a room ventilated by an air jet - the effect of turbulence model and wall function formulation, *Proc. of ROOMVENT-90*, Oslo, June, 1989
- [8] Ozoe, H, A. Mouri, M. Ohmuro, S. W. Churchill and N. Lior, Numerical calculations of laminar and turbulent natural convection in water in rectangular channels heated and cooled isothermally on the opposing vertical walls. *Int. J. Heat Mass Transfer* 28, pp.125-138, 1985
- [9] Henkes, R. A. W. M. and C. J. Hoogendoorn, Comparison of turbulence models for the natural convection boundary layer along a heated vertical plate, *Int. J. Heat Mass Transfer*, Vol.32, No.1, pp.157-169, 1989
- [10] Chen, Q., A. Moser, and A. Huber, Prediction of Buoyant, Turbulent Flow by a Low-Reynolds-Number $k-\epsilon$ Model, *ASHRAE Transactions* 1990, V.96, Pt.1
- [11] Patel, V.C., W. Rodi, & G. Scheuerer, Turbulence models for near wall and low Reynolds number flows: a review, *AIAA Journal*, Vol.23, No.9, pp.1308-1319, 1985
- [12] Lam, C. K. G. & K. Bremhorst, A Modified Form of $k-\epsilon$ Model for Predicting Wall Turbulence, *Journal of Fluids Engineering, ASME Transactions*, Vol.103, 1981, pp.456-460
- [13] Rosten, H. I. and D. B. Spalding, *The PHOENICS Reference Manual*, Chapter 6, CHAM TR/200, Oct. 1987, pp.6.91-6.92
- [14] Patankar, S. V. (1980) *Numerical Heat Transfer and Fluid Flow*, Chapter 7, pp.139 - 143., Hemisphere Publishing Corporation.
- [15] Khalifa, A.J.N. & R. H. Marshall, Validation of heat transfer coefficients on interior building surfaces using a real-sized indoor test cell, *J. Heat Mass Transfer*, Vol.33, No.10, pp.2219-2236, 1990
- [16] Hammond, G.P., Profile analysis of heat/mass transfer across the plane wall-jet, *Proceedings of the 7th international Heat Transfer Conference*, Munich, Vol.3, pp.349-355, 1982

